CHEMICAL ENGINEERING TRANSACTIONS

VOL. 48, 2016

A publication of AIDIC
The Italian Association of Chemical Engineering
Online at www.aidic.it/cet

Guest Editors: Eddy de Rademaeker, Peter Schmelzer

ISBN 978-88-95608-39-6; **ISSN** 2283-9216

DOI: 10.3303/CET1648032

Multicomponent Hydrocarbon Pool Fire: Analytical Modelling and Field Application

Bruno Fabiano[a]*, Carlo Caviglione[a], Andrea P. Reverberi[b], Emilio Palazzi[a]

[a] DICCA – Civil, Chemical and Environmental Engineering Department – Polytechnic School University of Genoa, Via Opera Pia, 15 – 16145 Genoa, Italy
[b] DCCI - Chemistry and Industrial Chemistry Department. - University of Genoa, via Dodecaneso 31, 16146 Genoa, Italy
brown@unige.it

In analyzing pool fires and the potential for domino effects, the evaluation of thermal radiation and issues of interplant spacing, employees' safety zones, fire wall specifications are to be addressed on the basis of a proper consequence analysis. Fire evolution can behave in different ways, according to the characteristics of the liquid pool and interactions with the surroundings. We face the modelization of an atypical scenario, consisting of a pool fire of coal tar, a multi-component mixture, with hydrocarbon components characterized by a broad range of normal boiling points, under semi-confined geometry. Analytical solution of energy and mass balances is approached by considering "hydrocarbon key components". A peculiar novelty of the approach is that the physical model of the pool is solved to provide a description of a variable heat emitting flame area, as a function of the vertical flame axis, up to a limiting value. In order to evidence the effective potentialities of the method, starting from a real accident in a coal industry, a detailed validation of the approach is performed making reference to a coal tar fire scenario embedded in a rectangular bund.

1. Introduction

Many survey on accidents in the process sectors, based on Major Hazards Incident Data System (MHIDAS) (Khan & Abbasi, (2000), Mannan (2005), or FACTS (Fabiano and Currò, 2012) evidenced that pool fire is present as one of the dominant evolving scenario (with an approximate figure of 42%). Additionally, among different fire scenarios, pool fire is by far the most frequent, covering more than 60% of all fire incidents (Persson & Lönnermark, 2004). A pool fire can occur when a flammable liquid is accidentally released on ground, or water, as a primary accidental event or following accident escalation (Lisi et al., 2015) and when a buoyancy-driven, turbulent non-premixed flame is formed above the pool upon ignition. This scenario differs from other types of fires by a very low initial momentum and by a tendency to be strongly influenced by buoyancy effects (Mannan, 2005). Even if scientific literature on pool-fire modeling is sparse, the usual approach considers circular geometry, pseudo steady-state conditions, uniform flame temperature, cylindrical/conical flame shape with height depending on pool diameter. Fire evolution can behave in different ways and, depending on the interactions with the surroundings, can exert both thermal and toxic hazards (Vianello et al., 2012). The specific analysis of rather complicated situations (partial confinement, irregular shapes, complex kinetics, heavy hydrocarbon fire, unsteady-state) usually requires the use of sophisticated integral models and/or CFD calculations. However, when conservative results are enough as a first screening tool, analytical models can be conveniently applied in hazard assessment (Fabiano et al., 2015), or to evaluate hazardous events posing a higher risk than the safety level and to determine safety measures (Abrahamsen et al., 2013). In this paper, we face the modelization of a pool fire of coal tar, a multi-component mixture, with hydrocarbon components characterized by a broad range of normal boiling points considering the peculiar burning behavior by proper simplifying hypotheses. The tars obtained either by low or high temperature coal carbonization of coal are complex mixtures of a myriad of aromatic compounds of widely ranging concentrations. The tar chemical nature and composition vary substantially with the parent coal rank, with a strong dependence on pyrolysis conditions (temperature, pressure, effect of different reactors (Solomon et al, 1992.) and more general pyrolysis environment (Chiarioni et al., 2006). Analytical solution of energy and

Please cite this article as: Fabiano B., Caviglione C., Curro' F., Palazzi E., 2016, Multicomponent hydrocarbon pool fire: primary and secondary effect modelling with enhanced view factor evaluation., Chemical Engineering Transactions, 48, 187-192 DOI:10.3303/CET1648032

mass balances is approached by considering "hydrocarbon key components" of the coal tar, resulting from tar sample analyses.

2. Model description

Pool fire development is described by considering the interactions among four sub-systems, namely liquid pool, flame region, flammable vapour region and atmosphere. The whole model is approached by simultaneously solving mass, energy and momentum balances. To the purpose of this study, we refer to the light components of coal tar, as resulting from chemical characterization on samples taken at different times from a coal dry distillation plant and summarized in Table 1.

Table 1: Chemical composition of actual coal tar.

Fuel (HC)	Molar mass (M_i)	Mol per mass unit ($\hat{n}_i$)				
		C	H_2	S	O_2	N_2
Benzene C_6H_6	78	0.077	0.039	-	-	-
Toluene C_7H_8	92	0.076	0.044	-	-	-
Naphtalene $C_{10}H_8$	128	0.079	0.031	-	-	-
Anthracene $C_{14}H_{10}$	178	0.079	0.028	-	-	-
Tar oil	128	0.073	0.035	$3.1 \cdot 10^{-4}$	$9.4 \cdot 10^{-4}$	$3.6 \cdot 10^{-4}$

2.1 Combustion stoichiometry

As well known, a pool fire is sustained through the supply of sufficient oxidants for combustion by the air entraining into the flame region, so that oxygen plays a role determining maximum flame temperature and thermal power (Palazzi et al., 2014). In developing the mass balance of the combustion and considering as well the data summarized in Table 1, we must notice that reactants entrained from boundaries (oxygen and vaporized HC) and smoke products deriving from combustion itself are present within the flame region. Starting from Lewis and Von Elbe (1987), we shall consider two limiting oxygen molar fractions, y_{O_2} , namely, 0.10 and 0.12. Dealing with hydrocarbon oxidation, we shall consider as reference for fractional conversion, X, the value 0.9 suggested for large pool fire and for the radiating heat fraction the value 1 according to a conservative estimate. By indicating with $\hat{n}_a$ the air moles per unit mass of hydrocarbon entrained into the flame, we summarize the mass balances pertaining to this region in Table 2.

Table 2: Mass balance within the flame region F of the pool-fire.

Compound	Mol of i compound [$kmol_i/kg_{HC}$]		
	Entrained mol ($\hat{n}_{i,e}$)	Generated mol ($\hat{n}_{i,g}$)	Mol in the flame ($\hat{n}_i$)
Fuel (HC)	$\hat{n}_{HC} = 1/M_{HC}$	$-\hat{n}_{HC} X$	$\hat{n}_{HC}(1 - X)$
O_2	$0.21 \cdot \hat{n}_a$	$(\hat{n}_{O_2} - \hat{n}_C - ½\hat{n}_{H_2} - \hat{n}_S)X$	$0.21\hat{n}_a (\hat{n}_C + ½\hat{n}_{H_2} - \hat{n}_{O_2} + \hat{n}_S)X$
N_2	$0.79 \cdot \hat{n}_a$	$\hat{n}_{N_2} X$	$0.79\hat{n}_a + \hat{n}_{N_2} X$
CO_2	-	$\hat{n}_C X$	$\hat{n}_C X$
H_2O	-	$\hat{n}_{H_2} X$	$\hat{n}_{H_2} X$
SO_2	-	$\hat{n}_S X$	$\hat{n}_S X$
Total	$\hat{n}_{HC} + \hat{n}_a$	$(-\hat{n}_{HC} + \hat{n}_{O_2} + ½\hat{n}_{H_2} + \hat{n}_{N_2})X$	$\hat{n}_{HC} + \hat{n}_a - (\hat{n}_{HC} - \hat{n}_{O_2} - ½\hat{n}_{H_2} - \hat{n}_{N_2})$

Hence, the molar fraction of oxygen and the specific air moles in the flame region are respectively calculated:

$$y_{O_2} = \frac{0.21\hat{n}_a - \left(\hat{n}_c + \frac{1}{2}\hat{n}_{H_2} + \hat{n}_S - \hat{n}_{O_2}\right)X}{\hat{n}_a + \hat{n}_{HC}(1-X) + \left(\hat{n}_{O_2} + \hat{n}_{N_2} + \frac{1}{2}\hat{n}_{H_2}\right)X} \quad (1)$$

$$\hat{n}_a = \frac{y_{O_2}\left[\hat{n}_{HC}(1-X) + \left(\hat{n}_{O_2} + \hat{n}_{N_2} + \frac{1}{2}\hat{n}_{H_2}\right)X\right] + \left(\hat{n}_c + \frac{1}{2}\hat{n}_{H_2} + \hat{n}_S - \hat{n}_{O_2}\right)X}{0.21 - y_{O_2}} \quad (2)$$

By assuming in each flame section the validity of the following relationships among the air flow rate, $\dot{m}_a$, entrained hydrocarbon vapours, $\dot{m}_v$, and total mass flow rate, $\dot{m}$, :

$$\dot{m}_a = M_a \hat{n}_a \dot{m}_v \quad (3)$$

$$d\dot{m} = d\dot{m}_v + d\dot{m}_a = (1 + M_a\hat{n}_a)d\dot{m}_v \quad (4)$$

we obtain the following equations:

$$\dot{m}_a = \frac{1}{K}\dot{m} \quad (5) \qquad \dot{m}_v = \frac{K-1}{K}\dot{m} \quad (6)$$

$$K = \frac{\dot{m}}{\dot{m}_a} = 1 + \frac{1}{M_a\hat{n}_a} \quad (7)$$

2.2 Fluid-dynamic considerations

The reference model of the pool-fir and ideal physical domains involved in fire behavior is depicted in Fig. 1.

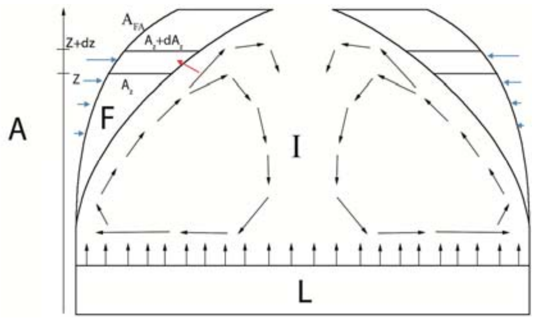

Figure 1: Physical model of the flame in wind absence (L=pool; V=vapour; F = flame; I=intermediate).

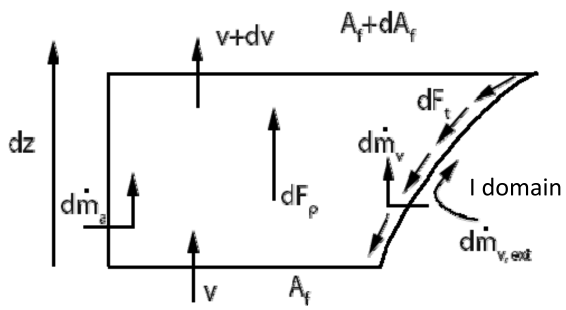

Figure 2: Flame element (dV=Adz) interactions.

We can observe that, for increasing z values starting from the floor level, the smoke flow rate increases and, correspondingly, the area of the section of the advecting smoke, A_z. Due to reactant depletion in the outer part of the flame and to the entrainment of non-reacted hydrocarbons (HC) from the inner part of the flame, this section tends to move towards the pool center as z increases. This trend is also connected to the radial component of the momentum of the entrained reactants (air and HC), which is directed towards the pool center. The mono-dimensional modeling is faced starting from mass and vertical component momentum balances referred to the flame element in Fig. 2. As working hypotheses, we assume that the external boundary of the flame be constant: $P_A(z) = P_r$ and that the interface surface be a parallelepiped with vertical, or inclined axis ($A_{FA} = P_r h$ in wind absence). If we assume, according with Raj (2007), that the global HC mass entrained into the flame be proportional to the ascending velocity of the gases within the flame core, it follows that only a fraction $d\dot{m}_{HC,F}$ can enter into *dz* and contribute to the flame development within the region F, while the remaining part of the entrained HC, $d\dot{m}_{HC,I}$, will touch on the flame still remaining into I domain.

$$d\dot{m}_{HC} = d\dot{m}_a = f\rho v P_r dz \quad (8)$$

$$d\dot{m}_{HC,F} = d\dot{m}_v = (K-1)d\dot{m}_a \quad (9)$$

$$d\dot{m}_{HC,I} = (2-K)d\dot{m}_a = (2-K)f\rho v P_r dz \quad (10)$$

The mass and momentum balances referred to the flame can be written as:

$$d\dot{m} = Kd\dot{m}_a = Kf\rho vP_r dz \quad (11) \qquad d\dot{M}_z = (\rho_a - \rho)gA_z dz - (2-K)f\rho v^2 P_r dz \quad (12)$$

The simultaneous integration of mass and momentum balances yields the ascending velocity, *v,* the flame surface, A_z, the air flow rate and the HC flow rate by the following analytical expressions:

$$v = \eta z^{1/2} \quad (13) \qquad A_z = \frac{2}{3}\frac{\delta}{\rho} z \quad (14)$$

$$\dot{m}_a = \frac{2}{3}\frac{1}{K}\delta\eta z^{3/2} \quad (15) \qquad \dot{m}_v = \frac{2}{3}\frac{K-1}{K}\delta\eta z^{3/2} \quad (16)$$

where: $\delta = Kf\rho P_r$ $\qquad \eta = \left(\frac{2K}{K+6}\vartheta\right)^{1/2}$ $\qquad \vartheta = \left(\frac{\rho_a}{\rho} - 1\right)g$

Compared with a previous model (Palazzi and Fabiano, 2012), the above equations allow evaluating the dependence of the flame parameters upon the vertical coordinate z. Additionally, the effects of non-complete oxidation of HC entrained into the flame, as well as the dimensions of the region I corresponding to the residual HC cloud following flame extinguishing, are properly taken into account by means of K parameter, defined according to Eq. (7). A further refinement would require proper regularization techniques (e.g. Reverberi et al., 2013), which is out of the purpose of the current simplified approach.

2.3 Thermodynamic considerations

The flame energy balance can be expressed as:

$$\Delta\dot{H}_u + \Delta\dot{H}_c = \dot{Q}_{FA} \quad (17)$$

where: $\Delta\dot{H}_u = \dot{m}_v \sum \Delta\tilde{H}_i \hat{n}_i$ (18) $\qquad \Delta\dot{H}_c = \Delta\hat{H}_{c,298}\dot{m}_v X$ (19) $\qquad \dot{Q}_{FA} = \dot{q}''_F A_{FA} = \dot{q}''_F P_r h$ (20)

By substituting the relevant expressions into Eq. (17), one can write:

$$\dot{m}_v \Delta\hat{H} = \dot{q}''_F P_r h \quad (21)$$

where: $\Delta\hat{H} = \sum \Delta\tilde{H}_i \hat{n}_i + \Delta\hat{H}_{c,298} X$ (22) $\qquad \dot{q}''_F = -\varepsilon\sigma T^4$ (23)

being ε the flame emissivity and σ = $5.67\cdot10^{-11}$ kW m^{-2} K^{-4} the Stephan-Boltzmann constant.
Assuming that the pool radiating energy be completely utilized for the vaporization of the liquid hydrocarbons, we get the vapour mass flow rate as follows:

$$\dot{m}_v = -\frac{\dot{q}''_F A_v}{\Delta\hat{H}_v} \quad (24)$$

By combining Eqs.(20) and (23), one can write:

$$h(T) = \frac{A_v}{P_r}\frac{-\Delta\hat{H}}{\Delta\hat{H}_v} \quad (25)$$

By substituting Eqs.(23) and (24) into Eq.(15), at the limiting height for flame extinguishing, *z*=*h*, it follows:

$$\frac{-\dot{q}''_F A_v}{\Delta\hat{H}_v} = \frac{2}{3}\frac{K-1}{K}\delta\eta\left(\frac{A_v}{P_r}\frac{-\Delta\hat{H}}{\Delta\hat{H}_v}\right)^{3/2} \quad (26)$$

At last, from Eq. (26) we obtain:

$$-\dot{q}''_F = \frac{2}{3}(K-1)\eta f\rho\left(\frac{A_v}{P_r}\frac{1}{\Delta\hat{H}_v}\right)^{1/2}\left(-\Delta\hat{H}\right)^{3/2} = \beta(T) \quad (27)$$

Finally, it is possible to calculate numerically the temperature T from the last equation, having properly accounted for the dependence of $\dot{q}''_F$ and ρ upon temperature, by pertinent formulae. By applying Eq. (24) and (25) one can easily obtain the corresponding values of $\dot{m}_v$,*h* and, subsequently, of all relevant parameters.

3. Results and discussion

An important feature of tank pool fire is that the targets of interest can include other units, such as tanks, gas pipes and storage sites. Starting from a real accident in a downstream oil industry involving pool fire of a heavy liquid HC mixture, we present the application to an industrial case study in order to evidence the effective potentialities of the method. Reference is made to a coal tar fire scenario retained within a rectangular domain with dimensions 21 x 24 m, assuming the previously defined key components of coal tar. Equations (27), (24), (25) and (34) practically concern the essential features of our model and, to the end of this study, they allow calculating the values of the other source parameters T and h required to estimate the risk of exposure to the thermal radiation. As widely reported, once initiated, the fire can behave in different ways, according to the characteristics (size, shape, temperature and composition) of the liquid pool and the possible interactions with the surroundings (confinement, windy or calm environment, etc.). In this model we considered the time dependent increase of the vaporization rate of the different HC components; the formation and rise of a column of hot gases, favoring fresh air entrainment and mixing with HC vapours and, after all, the fire power increase. Moreover, we evaluated the temperature increase up to a level determined from the balance between the previously mentioned power and the heat transferred to the environment, particularly as sensible heat of the fumes and by radiation. According to the model, a variable heat emitting flame area is calculated as a function of the vertical flame axis, up to the maximum limiting height, *z=h*. It must be remembered that, especially under windy conditions, escalation in pool fire is always possible and that the severity of fires impacting on a target is therefore a critical issue influencing the dynamic temperature profile of involved plant section. In the modelization, we included a novel numerical development of view factors in order to describe heat radiation received by a target, with fully random angles between the heat emitting and receiving surfaces. The qualitative description of flame "tilt-drag", with or without obstacle confinement is provided in Fig. 3: C C'_d and CC' are respectively the theoretical trend and the simplified line of the flame axis in obstacle absence, while CC*C'' is a more realistic description considering the actual situation with obstruction.

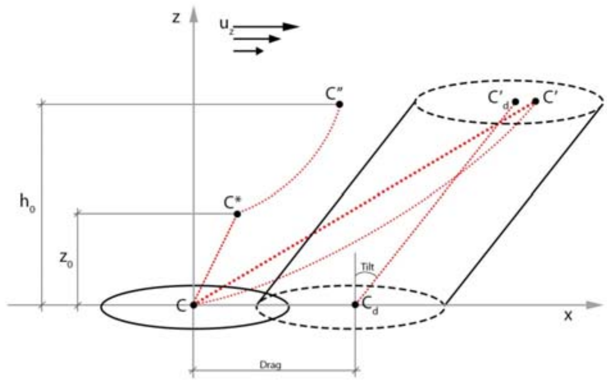

Figure 3: Physical model of the flame tilt and drag.

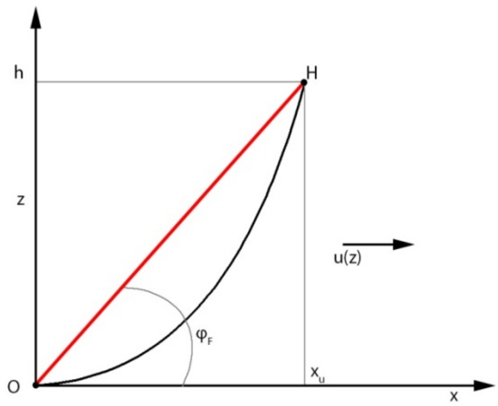

Figure 4: Simplified flame tilt model.

The first step, here described (Fig. 4), is the development of a plane flame tilt, based upon mass and vertical momentum balances referred to the flame element depicted in the previously mentioned Fig. 2. By proper straightforward calculations, the flame axis CC' is conservatively obtained as follows, being p the pool perimeter and u_0 the reference wind velocity at the height z_0:

$$x = \frac{\psi u_0}{\eta} z^{(0.5+p)} \quad (28) \qquad \psi = \psi(p) = \frac{6}{(1+2p)(3+2p)z_0^p} \quad (29)$$

At the extinguishing height *h*, it follows:

$$x_h = x(h) = \frac{\psi u_0}{\eta} h^{(0.5+p)} \quad (30)$$

Under the simplifying assumption of plane flame with CC' axis, the corresponding tilt angle is calculated by:

$$\varphi_F = \arctan\left(\frac{h}{x_h}\right) = \arctan\left(\frac{\eta}{\psi u_0} h^{(0.5-p)}\right) \quad (31)$$

The maximum and minimum heat radiation at the target point (coal tar loading point at a minimum distance with potential man presence of 1 m) for different key elements and several atmospheric classes (Pasquill and Smith, 1983) are summarized in Table 3. In this table we consider the maximum and minimum values obtained from the different combination of the parameter (f, y_{02} , X and ε). From the above data, we can calculate the maximum allowable exposure time, t_{adm} , by an empirical relationship (Palazzi et al., 2013) in order to assess the possibility for an individual to survive a fire, e.g. by escaping into a safe location:

$$t_{adm} = 631 \cdot \dot{q}_i^{-4/3} \quad (32)$$

Table 3: Maximum and minimum values of thermal radiation on target for different stability classes.

Thermal radiation on target [kW m^{-2}]		A	B	C	D	E
Benzene	Max	44	50	59	71	78
	Min	16	18	22	26	29
Toluene	Max	48	54	64	77	85
	Min	17	20	24	29	31
Naphtalene	Max	45	50	59	71	79
	Min	16	18	22	27	29
Anthracene	Max	45	51	61	73	80
	Min	16	18	22	27	29
Tar oil	Max	48	53	63	76	84
	Min	17	20	24	28	31

4. Conclusions

The analytical pool fire model here presented appears relatively straightforward to use in order to assess heavy HC pool fire hazards, allowing a cautious estimate of flame geometric parameters and thermal power behavior. The geometry of the pool is dictated by the surroundings and even if the model was successfully applied to a rectangular pool, it can be easily adapted to investigate a broad range of scenarios, characterized by different geometric or environmental conditions. Results are comparable with integral model approach. Further model refinements include the effect of confinement and the presence of obstacles within the bundle.

References

Abrahamsen E.B., Asche F., Milazzo M.F., 2013, An evaluation of the effects on safety of using safety standards. Safety Science 59: 173-178.

Chiarioni A., Reverberi A.P., Fabiano B., Dovì V.G., 2006, An improved model of an ASR pyrolysis reactor for energy recovery. Energy 31, 2124-2132.

Fabiano B., Currò F., 2012, From a survey on accidents in the downstream oil industry to the development of a detailed near-miss reporting system, Process Safety and Environmental Protection 90, 357-367.

Fabiano B., Pistritto F., Reverberi A., Palazzi E., 2015, Ethylene–air mixtures under flowing conditions: a model-based approach to explosion conditions. Clean Technologies and Environmental Policy 17, 1261-1270 DOI: 10.1007/s10098-015-0966-1

Khan F. I., & Abbasi S. A., 2000, Risk analysis of a typical chemical industry using ORA procedure. Journal of Loss Prevention in the Process Industries 14, 43-59.

Lewis B., von Elbe G., Combustion, flames & explosions of gases, 3rd ed. Academic Press Inc., New York, 1987.

Lisi R., Consolo G., Maschio G., Milazzo M.F., 2015, Estimation of the impact probability in domino effects due to the projection of fragments. Process Safety and Environmental Protection 93, 99-110.

Mannan S. Lees' loss prevention in the process industries hazard identification, assessment, and control. Amsterdam: Elsevier Butterworth-Heinemann, 2005.

Palazzi E., Fabiano B. 2012. Analytical modelling of hydrocarbon pool fires: conservative evaluation of flame temperature and thermal power. Process Safety and Environmental Protection 90, 121-128.

Palazzi E., Currò F., Fabiano B. 2013. Accidental Continuous Releases from Coal Processing in Semi-Confined Environment. Energies 6(10), 5003-5022.

Palazzi E., Currò F., Reverberi A., Fabiano B. 2014. Development of a theoretical framework for the evaluation of risk connected to accidental oxygen releases. Process Safety Envir. Protection 92, 357-367.

Pasquill F., Smith F.B., Atmospheric diffusion, 3rd edition. John Wiley & Sons, New York, 1983.

Persson H., & Lönnermark A. 2004. Tank fires. SP report, 14.

Ray P.K, 2007. Large hydrocarbons fuel pool fires: physical characteristics and thermal emission variations with height. Journal of Hazardous Materials 140, 280–292.

Reverberi A.P., Fabiano B., Dovì, V.G., 2013, Use of inverse modelling techniques for the estimation of heat transfer coefficients to fluids in cylindrical conduits. Int. Comm. in Heat and Mass Transfer 42, 25-31.

Solomon P.R., Serio M.A., Suuberg E.M., 1992, Coal pyrolysis: experiments, kinetic rates and mechanisms Prog. Energy Combust. Sci. 18, 133-220.

Vianello C., Fabiano B., Palazzi E., Maschio G., 2012, Experimental study on thermal and toxic hazards connected to fire scenarios in road tunnels. J. of Loss Prevention in the Process Industries 25, 718-729.